



Contents lists available at ScienceDirect

Neurobiology of Aging

journal homepage: www.elsevier.com/locate/neuaging

Alzheimer's disease is associated with altered expression of genes involved in immune response and mitochondrial processes in astrocytes

Shobana Sekar^{a,b}, Jacquelyn McDonald^{a,b}, Lori Cuyugan^{a,b}, Jessica Aldrich^a, Ahmet Kurdoglu^a, Jonathan Adkins^{a,b}, Geidy Serrano^{b,c}, Thomas G. Beach^{b,c}, David W. Craig^a, Jonathan Valla^{b,d}, Eric M. Reiman^{a,b,c,e}, Winnie S. Liang^{a,b,*}

^a Neurogenomics Division, Translational Genomics Research Institute, Phoenix, AZ, USA

^b Arizona Alzheimer's Consortium, Phoenix, AZ, USA

^c Civin Laboratory of Neuropathology, Banner Sun Health Research Institute, Sun City, AZ, USA

^d Department of Biochemistry, Midwestern University, Glendale, AZ, USA

^e Banner Alzheimer's Institute, Phoenix, AZ, USA

ARTICLE INFO

Article history:

Received 25 July 2014

Received in revised form 26 September 2014

Accepted 27 September 2014

Keywords:

Alzheimer's disease

Posterior cingulate

Astrocytes

RNA sequencing

Immune response

Mitochondria

ABSTRACT

Alzheimer's disease (AD) is characterized by deficits in cerebral metabolic rates of glucose in the posterior cingulate (PC) and precuneus in AD subjects, and in APOEε4 carriers, decades before the onset of measurable cognitive deficits. However, the cellular and molecular basis of this phenotype remains to be clarified. Given the roles of astrocytes in energy storage and brain immunity, we sought to characterize the transcriptome of AD PC astrocytes. Cells were laser capture microdissected from AD (n = 10) and healthy elderly control (n = 10) subjects for RNA sequencing. We generated >5.22 billion reads and compared sequencing data between controls and AD patients. We identified differentially expressed mitochondria-related genes including *TRMT61B*, *FASTKD2*, and *NDUFA4L2*, and using pathway and weighted gene coexpression analyses, we identified differentially expressed immune response genes. A number of these genes, including *CLU*, *C3*, and *CD74*, have been implicated in beta amyloid generation or clearance. These data provide key insights into astrocyte-specific contributions to AD, and we present this data set as a publicly available resource.

© 2014 The Authors. Published by Elsevier Inc. This is an open access article under the CC BY-NC-ND license (<http://creativecommons.org/licenses/by-nc-nd/3.0/>).

1. Introduction

With the rapidly growing prevalence of Alzheimer's disease (AD), improved understanding of the molecular and cellular basis of the disease is needed to identify and develop improved diagnostics and treatments. Numerous imaging studies have set the stage for characterizing AD in live subjects. Using fluorodeoxyglucose position emission tomography (FDG-PET), researchers have characterized an association between AD and progressive reductions of cerebral metabolic rates of glucose (CMRgl) in both AD patients (Minoshima et al., 1997; Reiman et al., 1996, 2001, 2004) and young adult APOEε4 carriers 4 decades before the expected onset of

cognitive deficits (Reiman et al., 2004). Affected brain regions include the posterior cingulate (PC) and parietal, temporal, and frontal cortices (Alexander et al., 2002; Fox et al., 2000; Minoshima et al., 1997; Thal et al., 2006), with the PC and precuneus demonstrating the earliest metabolic deficits in AD (Minoshima et al., 1997; Reiman et al., 2004). Such deficits may be associated with metabolic dysfunctions in neurons or glial cells (Mark et al., 1997; Piert et al., 1996), reductions in the density or activity of terminal neuronal fields or perisynaptic glial cells (Magistretti and Pellerin, 1996; Schwartz et al., 1979), or a combination of both, and additionally highlights a metabolic role of the PC in AD.

In previous work, we identified widespread downregulated expression of electron transport and mitochondrial translocase genes in non-tangle bearing neurons microdissected from the PC of AD subjects (Liang et al., 2008a, 2008b). In a separate study, decreased cytochrome c oxidase activity was also identified across all 6 layers of the PC cortex in AD subjects (Valla et al., 2001). Although these findings provide evidence that mitochondrial

* Corresponding author at: Neurogenomics Division, Translational Genomics Research Institute, 445 N. Fifth Street, Phoenix, AZ 85004, USA. Tel.: +1 602 343 8731; fax: +1 602 343 8844.

E-mail address: wliang@tgen.org (W.S. Liang).

dysfunction may play a role in characteristic CMRgl deficits in AD, it is unclear as to what pathogenic contributions may be derived from astrocytes in the PC. Importantly, previous studies have shown that astrocytes demonstrate changes with respect to aging and AD. Examples include the occurrence of structural changes in astrocytes in the dentate gyrus of aged rats (Geinisman et al., 1978), distinct clustering of astrocytes and astroglial hypertrophy in the hippocampi of aged rats (Landfield et al., 1977), release of proinflammatory factors from astrocytes in AD (Akiyama et al., 2000), and buildup of beta amyloid (A β) molecules within astrocytes (Akiyama et al., 2000), which may result from deficits in the ability of the cell to degrade A β , and recent work suggesting that activation of glial cells may have a primary role in impacting the health of neurons in AD (Perez-Nievas et al., 2013). Given this previous research and astrocytes' roles in energy storage and metabolism (Pellerin and Magistretti, 1994; Tsacopoulos and Magistretti, 1996), immunity (Jensen et al., 2013), and the greater than 2-fold increase in the number of astrocytes compared with neurons in the human brain (Jensen et al., 2013; Nedergaard et al., 2003; Sherwood et al., 2006; Sofroniew and Vinters, 2010), we hypothesized that PC astrocytes demonstrate significant expression changes in AD. With the role of astrocytes in energy storage and metabolism, we further hypothesize that genes involved in mitochondrial processes are also dysregulated in AD PC astrocytes.

A number of studies have evaluated human and murine astrocyte transcriptomes using microarray technology (Cahoy et al., 2008; Hawrylycz et al., 2012; Simpson et al., 2011; Yasui et al., 2013) or focused approaches such as Northern blotting (Pasterneck et al., 1989) or real time polymerase chain reaction (PCR) (Zhao et al., 2011). Simpson et al. (2011) expression profiled glial fibrillary acidic protein (GFAP) positive astrocytes microdissected from the temporal cortex of elderly subjects and identified differentially expressed genes with respect to Braak stage and apolipoprotein (APOE) ϵ 4 carrier status. In a separate study, cortical astrocytes were collected from young and old mice and expression profiled to reveal altered expression of key genes involved in neuronal signaling (Orre et al., 2014). In this study, we used laser capture microdissection (LCM) to collect aldehyde dehydrogenase 1 family, member L1- (ALDH1L1) positive astrocytes from PC cortex in both AD subjects ($n = 10$) and healthy elderly controls ($n = 10$). GFAP was not used in our study because of a number of caveats with this marker including: (Minoshima et al., 1997) GFAP demonstrates varying levels of expression across different cell types and regions (Roelofs et al., 2005; Sofroniew, 2009; Sofroniew and Vinters, 2010), is expressed in other glial cells outside of astrocytes (Sofroniew and Vinters, 2010), is highly expressed in reactive astrocytes (Eng et al., 2000; Pekny and Pekna, 2004; Pekny et al., 1995; Sofroniew and Vinters, 2010), and is often not identifiable in healthy tissue (Sofroniew and Vinters, 2010). However, ALDH1L1 is more specific to astrocytes than GFAP, does not preferentially mark reactive astrocytes, is expressed in mature astrocytes, and demonstrates a wider pattern of expression compared with GFAP such that GFAP-positive cells make up a subset of ALDH1L1-positive cells (Eng et al., 2000; Pekny and Pekna, 2004; Pekny et al., 1995; Sofroniew and Vinters, 2010). It is also important to note that our previous analysis of PC neurons was limited by the use of microarrays that used predefined probes to target only nuclear-encoded, and not mitochondrially-encoded, genes. However, in our study here, we capitalize on current genomic technologies to perform an unbiased evaluation of all transcripts present in each sample and to take advantage of the increased analytical sensitivity and wide dynamic range associated with next generation sequencing. We thus performed next generation RNA sequencing (RNAseq) of

astrocyte total RNA and describe here the first reported sequencing data set of PC astrocytes in AD.

2. Methods

2.1. Sample acquisition

Postmortem brain samples were collected at the Banner Sun Health Research Institute's Brain and Body Donation Program from 10 clinically classified late-onset AD subjects (4 males and 6 females; 5 APOE ϵ 3/4 subjects and 5 APOE ϵ 4/4 subjects) with a mean age at death of 83.9 years and 10 no disease (ND) healthy elderly control subjects (6 males and 4 females; 5 APOE ϵ 3/4 subjects and 5 APOE ϵ 4/4 subjects) with a mean age of death of 85.1 years. Clinically confirmed AD subjects had Braak stages ranging from IV to VI (Braak and Braak, 1991) and neuritic plaque densities of frequent (McKhann et al., 1984). Control subjects had Braak stages ranging from I to IV, plaque densities ranging from zero to moderate, and were clinically confirmed to not demonstrate dementia. Samples were collected with a mean postmortem interval (PMI) of 2.42 hours from the PC cortex (Brodmann areas 23 and 31). Following dissection, samples were flash frozen, sectioned (10 μ m), and mounted on glass or PEN membrane slides (Carl Zeiss Microscopy; Thornwood, NY). Information for each subject is shown in Table 1. Total RNA was isolated from a single section from each subject using the Qiagen RNeasy kit to evaluate RNA integrity. Samples demonstrated Agilent Bioanalyzer RNA Integrity Number (RINs) between 7.4 and 9.4 such that all samples were used for downstream analyses.

2.2. Staining and laser capture microdissection

PC brain sections were rapidly stained with Alexa Fluor 350 conjugated ALDH1L1 (anti-Aldehyde Dehydrogenase 1 Family, Member L1) rabbit polyclonal antibody (ABIN882166; antibodies-online; Atlanta, GA) to identify astrocytes. For each section, antibody was diluted 1:100 in phosphate-buffered saline (PBS) with ProtectRNA RNase inhibitor (Sigma-Aldrich; St. Louis, MO). For staining, each section was first fixed in ice-cold acetone for 3 minutes, washed 3X with PBS with RNase inhibitor, and diluted ALDH1L1 antibody was applied and incubated in the dark on ice for 10 minutes. The section was then washed 3X with PBS with RNase inhibitor, followed by consecutive washes with molecular water, 70% ethanol, 95% ethanol, and 100% ethanol. The section was then allowed to dry at room temperature. For each subject, approximately 300 astrocytes were LCMed from PC cortex onto the caps of AdhesiveCap opaque tubes (Carl Zeiss Microscopy) using the PALM LCM System (Carl Zeiss Microscopy; Thornwood, NY). Examples of ALDH1L1+ astrocytes, as well as a pre- and post-LCMed astrocyte, are shown in Supplementary Fig 1. Extraction buffer (10 μ L) from the Arcturus PicoPure RNA Isolation Kit (Life Technologies; Grand Island, NY) was pipetted directly onto the cap and incubated at 42 °C for 30 minutes to create cell lysate. Lysates were collected by centrifugation at 800xg for 2 minutes and stored at –80 °C until all samples were microdissected.

2.3. RNA isolation

Total RNA was isolated from all cell lysates using the Arcturus PicoPure RNA Isolation Kit (Life Technologies; Grand Island, NY) following the manufacturer's protocol. DNase treatment was additionally performed during RNA isolation using the RNase-free DNase set (Qiagen; Valencia, CA) following Appendix A of the Arcturus PicoPure manufacturer's protocol.

Table 1
Subject information

| Sample | Gender | APOE | PMI (h) | Expired age (y) | Plaque density | Braak score | NIA-R |
|------------|--------|------|---------|-----------------|----------------|-------------|------------------|
| Control 1 | M | 3/3 | 3.25 | 80 | Sparse | II | Criteria not met |
| Control 2 | F | 3/3 | 2.25 | 82 | Zero | II | Criteria not met |
| Control 3 | F | 3/3 | 2.50 | 95 | Zero | III | Criteria not met |
| Control 4 | M | 3/3 | 2.66 | 78 | Zero | II | Criteria not met |
| Control 5 | F | 3/4 | 1.50 | 85 | Moderate | III | Criteria not met |
| Control 6 | M | 3/4 | 2.00 | 91 | Zero | IV | Criteria not met |
| Control 7 | M | 3/4 | 2.33 | 76 | Sparse | I | Criteria not met |
| Control 8 | F | 3/4 | 2.50 | 85 | Zero | III | Criteria not met |
| Control 9 | M | 3/3 | 3.00 | 82 | Zero | IV | Criteria not met |
| Control 10 | M | 3/4 | 1.87 | 97 | Zero | III | Criteria not met |
| AD 1 | F | 3/3 | 1.50 | 85 | Frequent | VI | High |
| AD 2 | M | 3/3 | 2.95 | 82 | Frequent | V | High |
| AD 3 | F | 3/3 | 2.15 | 84 | Frequent | V | High |
| AD 4 | M | 3/4 | 2.25 | 78 | Frequent | VI | High |
| AD 5 | F | 3/4 | 2.16 | 78 | Frequent | VI | High |
| AD 6 | F | 3/4 | 2.66 | 85 | Frequent | V | High |
| AD 7 | F | 3/4 | 2.70 | 89 | Frequent | VI | High |
| AD 8 | M | 3/4 | 3.92 | 79 | Frequent | V | High |
| AD 9 | M | 3/3 | 2.05 | 86 | Frequent | VI | High |
| AD 10 | F | 3/3 | 2.15 | 93 | Frequent | IV | Intermediate |

Key: AD, Alzheimer's disease; APOE, apolipoprotein; F, female; M, male; NIA-R, National Institute on Aging and Reagan Institute neuropathologic AD severity score; PMI, postmortem interval.

2.4. Library preparation

All isolated total RNA from each LCM collection was used to generate and linearly amplify cDNA using the Ovation RNAseq System v2 (Nugen; San Carlos, CA) following the manufacturer's protocol. This system uses a primer mix to initiate amplification from the 3' end of genes as well as throughout the entire transcriptome. Amplified cDNA was input into the TruSeq DNA Sample Preparation Kit v2 (Illumina; San Diego, CA) and sequencing libraries were generated following the manufacturer's protocol with the exception that 10 cycles of PCR was used for library enrichment. Final libraries were analyzed on a Bioanalyzer DNA 1000 chip (Agilent Technologies; Santa Clara, CA). Equimolar pools of libraries were created for sequencing and reassessed on the Bioanalyzer before sequencing.

2.5. Paired-end sequencing

Library pools were clustered onto Illumina v3 flowcells using the Illumina Truseq PE Cluster Kit v3 on the Illumina cBot. Clustered flowcells were sequenced by synthesis on the Illumina HiSeq2000 using Illumina's Truseq PE Cluster Kit v3 and Illumina's TruSeq SBS Kits v3 for paired 83 base pair read lengths.

2.6. Sequencing data analysis

Raw sequencing data in the form of BCL files were converted to FASTQ files using Illumina BCLConverter software. Data were aligned against the human reference genome (build 37) using TopHat1.2 (Trapnell et al., 2009, 2012) and Cufflinks (Trapnell et al., 2012) was used to assemble aligned reads into transcripts. HTSeq (<http://www-huber.embl.de/users/anders/HTSeq/doc/overview.html>) was used to generate a counts table from Cufflinks output and DESeq2 v1.4.0 (Anders and Huber, 2010) (<http://www.bioconductor.org/packages/devel/bioc/html/DESeq2.html>) was used to calculate normalized read counts for each gene and/or transcript and to perform expression analysis. To evaluate inter-sample variability, we performed Pearson correlation analyses in R using normalized counts across all samples to identify any outliers.

DESeq2 uses a generalized linear model to evaluate differential expression while accounting for biological variance and uses a Wald test statistic to evaluate significance. A DESeqDataSet object is created using HTSeq counts and the DESeq wrapper function is called to perform differential analyses. The fold change is determined by dividing the average normalized read counts of AD samples over control samples for each transcript. Independent filtering and Cook cutoff parameters were set to ON to remove outliers and genes with low normalized read counts. *p*-values were corrected using the Benjamini and Hochberg False Discovery Rate, and results were annotated using the Biomart online portal (<http://www.ensembl.org/biomart/martview>).

MetaCore from Thompson Reuters (v6.10 build 40,284) was used for GeneGo pathway analysis. Weighted gene co-expression network analysis (WGCNA) (Horvath et al., 2006; Zhang and Horvath, 2005) was performed on differentially expressed genes (corrected *p* < 0.05). Gene sets were loaded into the WGCNA R package, and annotation of generated modules was performed using DAVID (Dennis et al., 2003).

All data generated through this study are accessible through National Center for Biotechnology Information (NCBI) database of genotypes and phenotypes (dbGaP; accession phs000745.v1.p1).

2.7. Quantitative-polymerase chain reaction validation

Quantitative-polymerase chain reaction (qPCR) was performed to experimentally validate differentially expressed transcripts in 2 phases: first, qPCR was performed on total RNA from astrocytes microdissected from 3 control subjects and 3 AD subjects and second, across total RNA isolated from whole PC sections from all 20 sequenced subjects (during initial sample quality control analyses described in Section 2.1). For the first phase, validation was performed on cDNA synthesized and linearly amplified from LCMed astrocyte pools using the Nugen Ovation RNA-Seq System V2 kit. Additional remaining cDNA from original collections used for sequencing were used for validations for AD4, AD6, and ND9. Based on sample availability, newly microdissected astrocyte pools were collected for AD8, ND1, and ND2. Total RNA was isolated using the PicoPure RNA Isolation kit and was used to generate cDNA for validation using the Nugen Ovation RNA-Seq System V2 kit.

REV3-like, polymerase DNA directed, zeta, catalytic subunit (REV3L) was selected as a reference gene because it demonstrated consistent high expression (greater than 1000 normalized read counts in each of all 20 samples) in RNAseq data and also demonstrated the lowest variance across all 20 samples. For the second phase, remaining total RNA from initial sample quality control analyses

(Section 2.1) was used and cDNA was generated using Qiagen QuantiTect Reverse Transcription Assay. Primers were designed using Primer3 and validated by performing a dilution series using Clontech Human RNA from Takara Bio Inc (Kyoto, Japan) which was also reverse transcribed using the QuantiTect Reverse Transcription assay. Cq values were plotted against the log of the input to

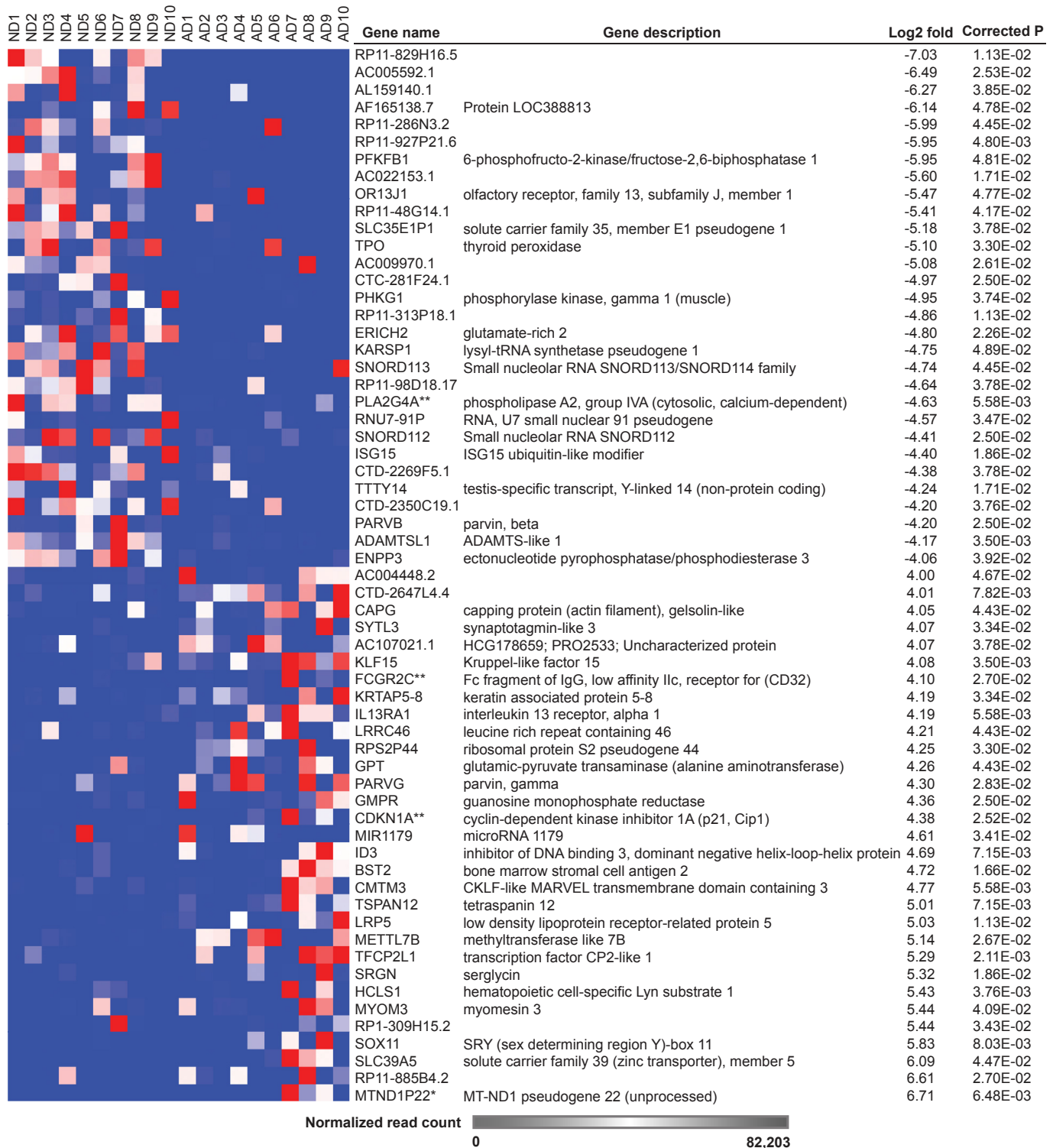


Fig. 1. Differentially expressed genes in AD PC astrocytes. Differentially expressed genes (corrected $p < 0.05$) with the highest log2-fold changes are shown. * represents mitochondrial gene; ** represents immune response gene. Abbreviations: AD, Alzheimer's disease; PC, posterior cingulate.

determine binding efficiency of each primer. QPCR reactions were performed in 10 μ L reactions using QuantiFast SYBR Green RT-PCR kit (Hilden, Germany) per the manufacturer's instructions on the Roche Lightcycler 480 system (Basel, Switzerland), with the exception that the initial reverse transcription step was omitted. Reactions were performed in triplicate with 1 nontemplate control.

3. Result and discussion

3.1. RNA sequencing

We sequenced 10 AD PC astrocyte pools and 10 ND (control) PC astrocyte pools to generate over 5.22 billion total reads and over 295 Gb of Q30 sequencing data. Both AD and ND groups were controlled for APOE genotype. An average of 123,214,013 mapped reads were sequenced per sample. Pearson correlation analyses on normalized read counts across all samples resulted in r values all greater than 0.88. All samples were thus included for differential expression analyses.

3.2. Differentially expressed genes in AD PC astrocytes

Comparison of AD samples with controls led to the identification of 226 differentially expressed genes (corrected $p < 0.05$; [Supplementary Table 1](#)). Genes demonstrating the greatest log₂-fold changes are shown in [Fig. 1](#). A total of 55.8% of significant genes demonstrated up regulated expression.

Differentially expressed genes include mitochondrial genes, defined as mitochondrially encoded genes or MitoCarta genes ([Pagliarini et al., 2008](#)) ([Table 2](#)). These genes include Fas-activated serine/threonine phosphoprotein kinase domains 2 (FASTKD2; log₂ ratio = −3.50), tRNA methyltransferase 61 homolog B (TRMT61B; log₂ ratio = −2.81), pitrilysin metalloproteinase 1 antisense RNA 1 (PREP/MP1; PITRM1-AS1; log₂ ratio = −3.20), NADH dehydrogenase (ubiquinone) 1 alpha subcomplex, 4-like 2 (NDUFA4L2; log₂ ratio = 3.23), and mitochondrially encoded NADH dehydrogenase 1 pseudogene 22 (MTND1P22; log₂ ratio = 6.71). FASTKD2, which localizes to the mitochondrial matrix, has been predicted to be involved in regulating apoptosis in breast cancer such that knockdown of the gene resulted in inhibition of apoptosis ([Yeung et al., 2011](#)). Homozygous nonsense mutations in FASTKD2 have also been previously reported in mitochondrial encephalomyopathy, a condition associated with decreased cytochrome c oxidase activity ([Ghezzi et al., 2008](#)). Decreased expression of FASTKD2 in AD PC astrocytes thus suggests perturbation of apoptosis regulation in these cells. TRMT61B, which also localizes to mitochondria, methylates adenosine at position 58 of cytoplasmic mitochondrial transport RNAs (tRNAs) and is hypothesized to improve processing, stability, or function of tRNAs

required for translation of respiratory factors ([Chujo and Suzuki, 2012](#)).

PITRM1/PREP/MP1 encodes an enzyme that is localized to the mitochondrial matrix ([Chow et al., 2009](#)) and that has been shown to degrade A β ([Falkevall et al., 2006](#)). Activity of this enzyme has also been reported to be decreased in the temporal lobe of AD subjects and transgenic AD murine brains ([Alikhani et al., 2011](#)). Decreased expression of a transcript antisense to PITRM1 may be associated with changes in regulation of PITRM1 expression. NDUFA4L2 has been reported to inhibit activity of complex I under hypoxic conditions through hypoxia-inducible transcription factor-1 (HIF-1) ([Tello et al., 2011](#)) such that its increased expression in AD PC astrocytes may impact complex I activity. Finally, we identified altered expression of a mitochondrially encoded pseudogene, MTND1P22. Pseudogenes, represented by DNA sequences that are similar to protein-coding genes but do not generate functional proteins, have historically been assumed to be nonfunctional but more recent research suggests that pseudogene transcripts may represent regulatory long noncoding RNAs ([Poliseno, 2012](#)). The differentially expressed mitochondrial pseudogene identified here is an unprocessed pseudogene, resulting from gene duplication, whereas processed pseudogenes result from a retrotransposition event ([Poliseno, 2012](#)). To date, there have been no reports of biological evidence of mitochondrially encoded pseudogenes, although nuclear-encoded mitochondrial pseudogenes are known ([Woischnik and Moraes, 2002](#)). Our understanding of these pseudogenes remains limited. However, given our current understanding of pseudogenes and the sequence similarity of this transcript with the NADH dehydrogenase 1 gene, MTND1P22 may have a role in transcription regulation. Additional differentially expressed mitochondrial genes include CTP synthase 2 (CTPS2; log₂ ratio = 3.15), mitochondrial ribosomal protein S2 (MRPS2; log₂ ratio = 2.88), methylenetetrahydrofolate dehydrogenase (NADP⁺ dependent) 2, methylenetetrahydrofolate cyclohydrolase (MTHFD2; log₂ ratio = −3.18), and transporter 1, ATP-binding cassette, subfamily B (TAP1; log₂ ratio = 2.83).

Pathway analysis of differentially expressed genes revealed that the most significantly impacted pathway in AD PC astrocytes is immune system response ([Table 3](#)) with 82.4% of significant genes in this pathway demonstrating upregulated expression in AD PC astrocytes. Furthermore, WGCNA, which performs functional organization of genes based on coexpression, on differentially expressed genes in AD astrocytes generated 7 coexpression modules, whereby the largest module ([Fig. 2A](#); turquoise module) demonstrated the highest DAVID enrichment scores for immune response and immune processes, including antigen processing and presentation and lymphocyte activation. Genes in each module are shown in [Fig. 2B](#). Given the role of astrocytes in central nervous system immunity under circumstances when insults are present

Table 2
Differentially expressed MitoCarta genes in AD PC astrocytes (corrected $p < 0.05$)

| Ensembl ID | Gene name | Description | Log ₂ -fold | p | Corrected p |
|-----------------|------------|---|------------------------|-----------------------|-----------------------|
| ENSG00000118246 | FASTKD2 | FAST kinase domains 2 | −3.67 | 6.41×10^{-8} | 1.37×10^{-3} |
| ENSG00000237399 | PITRM1-AS1 | PITRM1 antisense RNA 1 | −3.61 | 4.67×10^{-4} | 4.78×10^{-2} |
| ENSG00000065911 | MTHFD2 | Methylenetetrahydrofolate dehydrogenase (NADP ⁺ dependent) 2, methylenetetrahydrofolate cyclohydrolase | −3.18 | 2.95×10^{-4} | 3.93×10^{-2} |
| ENSG00000171103 | TRMT61 B | tRNA methyltransferase 61 homolog B (<i>Saccharomyces cerevisiae</i>) | −3.01 | 3.19×10^{-4} | 4.09×10^{-2} |
| ENSG00000168394 | TAP1 | Transporter 1, ATP-binding cassette, subfamily B (MDR/TAP) | 2.83 | 3.51×10^{-4} | 4.25×10^{-2} |
| ENSG00000122140 | MRPS2 | Mitochondrial ribosomal protein S2 | 2.88 | 6.84×10^{-5} | 2.40×10^{-2} |
| ENSG00000047230 | CTPS2 | CTP synthase 2 | 3.15 | 9.63×10^{-5} | 2.65×10^{-2} |
| ENSG00000185633 | NDUFA4L2 | NADH dehydrogenase (ubiquinone) 1 alpha subcomplex, 4-like 2 | 3.23 | 3.23×10^{-4} | 4.09×10^{-2} |
| ENSG00000251407 | MTND1P22 | MT-ND1 pseudogene 22 (unprocessed) | 6.71 | 5.14×10^{-6} | 6.48×10^{-3} |

Key: AD, Alzheimer's disease; PC, posterior cingulate; tRNA, transfer RNA.

Table 3
Pathway analysis of differentially expressed genes identified in AD PC astrocytes (corrected $p < 0.05$)

| # | Pathway/process | p | Ratio | Down (%) | Up (%) | Genes |
|----|--|-----------------------|--------|----------|--------|--|
| 1 | Immune system response | 4.21×10^{-5} | 21/970 | 17.6 | 82.4 | ARHGEF11, C3, CD74, CD81, CD93, CDKN1A, CLU, CYBB, FCGR2A, GSN, HLA-DRB1, IL13RA1, ISG15, PLA2G4A, PSMD4, TAP1, TNS1 |
| 2 | Hematopoiesis | 3.10×10^{-2} | 6/270 | 20.0 | 80.0 | CDKN1A, CYBB, FTL, TAP1, TPO |
| 3 | Transcription regulation | 1.48×10^{-1} | 1/18 | 0.0 | 100.0 | TBP |
| 4 | Vasoconstriction | 2.95×10^{-1} | 4/311 | 75.0 | 25.0 | ARHGEF11, OCLN, PHKG1, PLA2G4A |
| 5 | Calcium signaling | 3.31×10^{-1} | 5/430 | 50.0 | 50.0 | CDKN1A, HLA-DRB1, IL13RA1, P2RY6, PHKG1, PLA2G4A |
| 6 | Oxidative stress regulation | 4.04×10^{-1} | 6/578 | 14.3 | 85.7 | CYBB, FTL, HSF1, IL13RA1, PLA2G4A, RPS4X, SEPP1 |
| 7 | Blood clotting | 4.48×10^{-1} | 3/278 | 33.3 | 66.7 | FCGR2A, PLA2G4A, VKORC1 |
| 8 | Tissue remodeling and wound repair | 4.98×10^{-1} | 5/524 | 40.0 | 60.0 | CDKN1A, LRP5, OCLN, PLA2G4A, TGFA |
| 9 | Inflammatory response | 5.55×10^{-1} | 6/673 | 25.0 | 75.0 | CYBB, IL13RA1, PLA2G4A, TNS1 |
| 10 | Mitogenic signaling | 5.59×10^{-1} | 5/560 | 20.0 | 80.0 | CDKN1A, IGFBP5, IL13RA1, PLA2G4A, TGFA |
| 11 | Obesity | 5.64×10^{-1} | 2/212 | 0.0 | 100.0 | CDKN1A, TNS1 |
| 12 | Myogenesis regulation | 5.72×10^{-1} | 1/95 | 0.0 | 100.0 | CDKN1A |
| 13 | Vasodilation | 5.79×10^{-1} | 3/337 | 66.7 | 33.3 | ARHGEF11, FOSB, PHKG1 |
| 14 | Vitamin and cofactor metabolism and its regulation | 5.91×10^{-1} | 6/697 | 33.3 | 66.7 | ENPP3, FTL, MTHFD2, PHPT1, SCARB1, VKORC1 |
| 15 | Lipid biosynthesis and regulation | 6.43×10^{-1} | 3/370 | 100.0 | 0.0 | PLA2G4A |
| 16 | Cystic fibrosis disease | 6.75×10^{-1} | 5/636 | 14.3 | 85.7 | ANXA2, CYBB, FOSB, PSMD4, RAE8A, TAP1, TGFA |
| 17 | Vascular development (angiogenesis) | 6.89×10^{-1} | 4/522 | 25.0 | 75.0 | CDKN1A, MKNK2, PLA2G4A, VHL |
| 18 | Protein degradation | 6.94×10^{-1} | 2/269 | 0.0 | 100.0 | CDKN1A, HSF1 |
| 19 | Nucleotide metabolism and its regulation | 6.97×10^{-1} | 3/401 | 33.3 | 66.7 | CTPS2, ENPP3, GMPR |
| 20 | Cell differentiation | 7.25×10^{-1} | 7/922 | 57.1 | 42.9 | CDKN1A, FOSB, IL13RA1, NOTCH3, OCLN, PHKG1, PLA2G4A |

Key: AD, Alzheimer's disease; PC, posterior cingulate.

(Jensen et al., 2013), identification that immune system response processes are the most heavily perturbed pathways in AD PC astrocytes correlates with known astrocyte functions. These changes may be associated with activation of astrocytes in response to one or all the following: the presence of beta-amyloid, weakening of the blood-brain barrier (BBB), and exposure of sequenced cells to inflammatory cytokines.

Differentially expressed immune system response genes include clusterin (CLU), apolipoprotein J (APOJ) (log2 ratio = 1.97), complement component 3 (C3; log2 ratio = 2.82), and cluster of differentiation 74 molecule, major histocompatibility complex, class II invariant chain (CD74; log2 ratio = 3.52). Two large genome-wide association studies that evaluated over 23,000 individuals implicated an SNP, rs11136000, in CLU that is associated with late-onset AD (Harold et al., 2009; Lambert et al., 2009). CLU encodes a heterodimeric chaperone that has been found to inhibit A β oligomer uptake in human astrocytes (Mulder et al., 2014) such that increased expression of this gene in AD PC astrocytes may affect A β clearance. C3 encodes a member of the complement system, and this gene has been reported to demonstrate an age-related increase in expression in control (C57BL/6) mice with more significant increases in transgenic amyloid precursor protein (APP) mice during formation of A β (Reichwald et al., 2009). Finally, we identified upregulated expression of CD74 in AD PC astrocytes. CD74, which is involved in antigen presentation to T cells during an immune response, has also been found to interact with A β and obstruct A β production in HeLa cells (Matsuda et al., 2009). Upregulated expression of CD74 in AD PC astrocytes may thus represent an effect resulting from multiple causes encompassing both immune system and A β responses. Notably, the immune system response genes described here have all been shown to be associated with APP/A β such that APP/A β may be a key initiating factor in immune response pathways. Of relevance, the proximity of LCMed astrocytes to A β plaques was not evaluated during microdissection, but the findings reported here may be influenced by the higher plaque load in the AD subjects.

3.3. Experimental validation of differentially expressed genes

Based on sample availability, qPCR experiments were performed to validate expression changes. qPCR was first performed across 3 control and 3 AD subjects using cDNA generated from total RNA isolated from microdissected PC astrocytes to validate gene expression changes of 7 selected differentially expressed genes, or transcripts, identified through the AD versus ND comparison (Supplementary Fig. 2A and B). These genes and/or transcripts include RP11-488L18.10, RP11-797H7.1, TRMT61B, PPP5C, C3, TBP, and CLU. Because of limited availability of these samples, we also performed qPCR validation on total RNA that was isolated from an entire PC section from each subject during initial sample quality control analyses ($n = 20$; Supplementary Fig. 2A and C). These analyses were performed on 6 selected differentially expressed genes including TRMT61B, CTPS2, NDUF4AL2, CD74, CLU, and C3. Overall, the directionality of expression changes was validated across all genes. Notably, CLU and C3, both of which were evaluated by qPCR in microdissected astrocytes and whole PC sections, demonstrated larger increases in the astrocyte-specific data and lower increases in whole PC sections to show that the astrocyte-specific signal is diluted in whole PC sections.

4. Conclusions

In this study, we identified altered expression of mitochondrial and immune system response genes in PC astrocytes in the context of AD. Based on WGCNA and pathway analyses, immune response processes appear to be most heavily impacted in PC astrocytes in AD subjects. These results provide evidence that brain immunity and mitochondrial functions in PC astrocytes are perturbed in AD.

Given the role of astrocytes as immune sensors in the brain (Jensen et al., 2013), these cells may represent a first line of defense in response to insults, which may include inflammation, injury, or infection. Differentially expressed immune response genes in AD subjects include numerous genes that have been previously implicated as having key roles associated with A β production and clearance. However, it remains to be clarified if alterations in

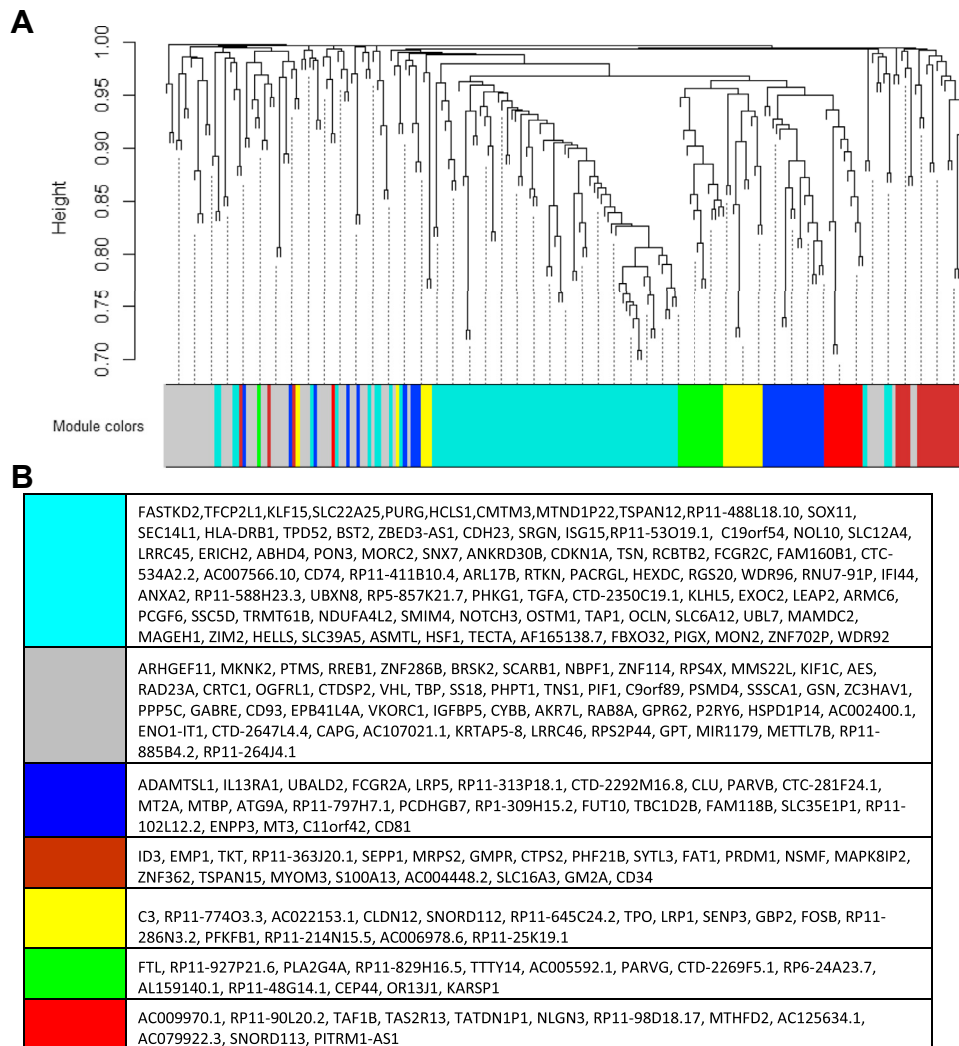


Fig. 2. WGCNA dendrogram of differentially expressed genes in AD PC astrocytes. A total of 226 differentially expressed genes (corrected $p < 0.05$) were used for WGCNA. (A) Seven coexpression modules were generated, and the total genes for each module are as follows: blue = 26, brown = 22, green = 14, gray = 53, red = 12, turquoise = 83, and yellow = 16. Each open-ended arm in the dendrogram represents a separate gene. (B) Genes falling within each module are listed. Abbreviations: AD, Alzheimer's disease; PC, posterior cingulate; WGCNA, Weighted gene coexpression network analysis.

immunity pathways parallel, overlap, or potentially precede, A β formation. Deeper investigations into young pre-AD and MCI (mild cognitive impairment) subjects will be needed to determine if immune response processes are similarly affected before onset of AD, and if perturbation of immune response pathways coincides with CMRgl deficits seen in young APOE ϵ 4 carriers. Likewise, additional regional analyses are needed to evaluate if immune response pathways are also heavily impacted in brain regions differentially affected by AD.

Although this study lends new insight into astrocytic changes in AD, we are limited by a few caveats. Although microdissection was used to collect astrocytes for sequencing, it is possible that fragments of adjacent endothelial cells or neurons may have also been collected. To mitigate this possibility, astrocytes were individually collected, but it is possible that astrocytic end feet may have been missed. As a secondary confirmation, we evaluated GFAP expression and identified increased expression in AD subjects (uncorrected $p = 1.63 \times 10^{-3}$, log2 fold = 2.49), as expected because of upregulation of GFAP in reactive astrocytes in AD (Eng et al., 2000; Panter et al., 1985; Sofroniew and Vinters, 2010), although we did not specifically collect GFAP-positive cells. Another limitation is

that we do not know the mitochondrial content of the microdissected cells, whereby differential expression of mitochondrial genes may reflect differential mitochondrial loads. Differences in mitochondrial content in both astrocytes and neurons in the context of AD have yet to be investigated. Third, it is not known if increased expression of mitochondrial genes directly translates to activation of energy metabolism pathways.

This study is also prefaced by significant region-specific transcriptional analyses in AD that have demonstrated discrete alterations in different areas of the brain. Key upregulated and downregulated genes have been identified in the amygdala and cingulate cortex of postmortem AD brains, correlating to processes including inflammation and energy metabolism, respectively (Loring et al., 2001). Although analyses were performed on whole tissue, upregulation of inflammation genes and downregulation of energy metabolism genes parallel our findings here, in addition to our previous report of decreased expression of electron transport genes in PC neurons (Liang et al., 2008a, 2008b). In a separate study, microarray analysis of LC Med CA1 hippocampal gray matter from formalin fixed paraffin embedded (FFPE) sections of AD brains suggests that increased expression of glial transcription factors

genes, among others, may be concentrated in white, and not gray, matter (Blalock et al., 2011). Although transcriptional analysis of FFPE samples may be associated with decreased specificity, this study provides evidence of divergent expression changes also at the level of gray and white matter. In neuron-specific transcriptomic studies in AD, key expression alterations were also identified across multiple brain regions, including the PC, hippocampal CA1, and middle temporal gyrus, in cortical neurons (Liang et al., 2008a, 2008b, 2010).

Such findings emphasize the need to consider cell-specific responses, roles, and contributions to AD pathogenesis. The benefits of RNAseq support our ability to perform cell-specific analyses by widening the dynamic range for transcript detection and by supporting an unbiased evaluation of all transcripts in a sample. Furthermore, identification of differentially expressed mitochondrial and immune response genes, and the respective roles of these genes in A β generation and clearance, lends valuable insight into previously uncharacterized cells in the PC. As we continue to improve our understanding of the discrete molecular events that occur in the PC in AD, we will strengthen our ability to identify potential targets for slowing and arresting disease progression at earlier stages of AD.

Acknowledgements

The authors thank Drs Carol Barnes and Matthew Huentelman and the Arizona Alzheimer's Consortium and the Arizona Alzheimer's Disease Core Center for supporting this study. This study was funded by NIH P30AG019610 through the Arizona Alzheimer's Disease Core Center pilot program. They additionally thank the participating subjects and families, Cynthia Lechuga, and Dr Kendall Jensen for support and assistance, and St. Joseph's Medical Center and Hospital for LCM access.

Appendix A. Supplementary data

Supplementary data associated with this article can be found, in the online version, at <http://dx.doi.org/10.1016/j.neurobiolaging.2014.09.027>.

References

- Akiyama, H., Arai, T., Kondo, H., Tanno, E., Haga, C., Ikeda, K., 2000. Cell mediators of inflammation in the Alzheimer disease brain. *Alzheimer Dis. Assoc. Disord.* 14 (Suppl 1), S47–S53.
- Alexander, G.E., Chen, K., Pietrini, P., Rapoport, S.I., Reiman, E.M., 2002. Longitudinal PET evaluation of cerebral metabolic decline in dementia: a potential outcome measure in Alzheimer's disease treatment studies. *Am. J. Psychiatry* 159, 738–745.
- Alikhani, N., Guo, L., Yan, S., Du, H., Pinho, C.M., Chen, J.X., Glaser, E., Yan, S.S., 2011. Decreased proteolytic activity of the mitochondrial amyloid-beta degrading enzyme, PreP peptidase, in Alzheimer's disease brain mitochondria. *J. Alzheimers Dis* 27, 75–87.
- Anders, S., Huber, W., 2010. Differential expression analysis for sequence count data. *Genome Biol.* 11, R106.
- Blalock, E.M., Buechel, H.M., Popovic, J., Geddes, J.W., Landfield, P.W., 2011. Microarray analyses of laser-captured hippocampus reveal distinct gray and white matter signatures associated with incipient Alzheimer's disease. *J. Chem. Neuroanat.* 42, 118–126.
- Braak, H., Braak, E., 1991. Neuropathological staging of Alzheimer-related changes. *Acta Neuropathol.* 82, 239–259.
- Cahoy, J.D., Emery, B., Kaushal, A., Foo, L.C., Zamanian, J.L., Christopherson, K.S., Xing, Y., Lubischer, J.L., Krieg, P.A., Krupenko, S.A., Thompson, W.J., Barres, B.A., 2008. A transcriptome database for astrocytes, neurons, and oligodendrocytes: a new resource for understanding brain development and function. *J. Neurosci* 28, 264–278.
- Chow, K.M., Gakh, O., Payne, I.C., Juliano, M.A., Juliano, L., Isaya, G., Hersch, L.B., 2009. Mammalian ptilin: substrate specificity and mitochondrial targeting. *Biochemistry* 48, 2868–2877.
- Chujo, T., Suzuki, T., 2012. Trmt61B is a methyltransferase responsible for 1-methyladenosine at position 58 of human mitochondrial tRNAs. *RNA* 18, 2269–2276.
- Dennis Jr., G., Sherman, B.T., Hosack, D.A., Yang, J., Gao, W., Lane, H.C., Lempicki, R.A., 2003. DAVID: database for annotation, visualization, and integrated discovery. *Genome Biol.* 4, P3.
- Eng, L.F., Ghimikar, R.S., Lee, Y.L., 2000. Glial fibrillary acidic protein: GFAP-thirty-one years (1969–2000). *Neurochem. Res.* 25, 1439–1451.
- Falkevall, A., Alikhani, N., Bhushan, S., Pavlov, P.F., Busch, K., Johnson, K.A., Eneqvist, T., Tjernberg, L., Ankarcrona, M., Glaser, E., 2006. Degradation of the amyloid beta-protein by the novel mitochondrial peptidase, PreP. *J. Biol. Chem.* 281, 29096–29104.
- Fox, N.C., Cousens, S., Scallan, R., Harvey, R.J., Rossor, M.N., 2000. Using serial registered brain magnetic resonance imaging to measure disease progression in Alzheimer disease: power calculations and estimates of sample size to detect treatment effects. *Arch. Neurol.* 57, 339–344.
- Geinisman, Y., Bondareff, W., Dodge, J.T., 1978. Hypertrophy of astroglial processes in the dentate gyrus of the senescent rat. *Am. J. Anat.* 153, 537–543.
- Ghezzi, D., Saada, A., D'Adamo, P., Fernandez-Vizarra, E., Gasparini, P., Tiranti, V., Elpeleg, O., Zeviani, M., 2008. FASTKD2 nonsense mutation in an infantile mitochondrial encephalomyopathy associated with cytochrome c oxidase deficiency. *Am. J. Hum. Genet.* 83, 415–423.
- Harold, D., Abraham, R., Hollingworth, P., Sims, R., Gerrish, A., Hamshere, M.L., Pahwa, J.S., Moskvina, V., Dowzell, K., Williams, A., Jones, N., Thomas, C., Stretton, A., Morgan, A.R., Lovestone, S., Powell, J., Proitsi, P., Lupton, M.K., Brayne, C., Rubinsztein, D.C., Gill, M., Lawlor, B., Lynch, A., Morgan, K., Brown, K.S., Passmore, P.A., Craig, D., McGuinness, B., Todd, S., Holmes, C., Mann, D., Smith, A.D., Love, S., Kehoe, P.G., Hardy, J., Mead, S., Fox, N., Rossor, M., Collinge, J., Maier, W., Jessen, F., Schürmann, B., Heun, R., van den Bussche, H., Heuser, I., Kornhuber, J., Wiltfang, J., Dichgans, M., Fröhlich, L., Hampel, H., Hüll, M., Rujescu, D., Goate, A.M., Kauwe, J.S., Cruchaga, C., Nowotny, P., Morris, J.C., Mayo, K., Sleegers, K., Bettens, K., Engelborghs, S., De Deyn, P.P., Van Broeckhoven, C., Livingston, G., Bass, N.J., Gurling, H., McQuillin, A., Gwilliam, R., Deloukas, P., Al-Chalabi, A., Shaw, C.E., Tsolaki, M., Singleton, A.B., Guerreiro, R., Mühleisen, T.W., Nöthen, M.M., Moebus, S., Jöckel, K.H., Klopp, N., Wichmann, H.E., Carrasquillo, M.M., Pankratz, V.S., Younkin, S.G., Holmans, P.A., O'Donovan, M., Owen, M.J., Williams, J., 2009. Genome-wide association study identifies variants at CLU and PICALM associated with Alzheimer's disease. *Nat. Genet.* 41, 1088–1093.
- Hawrylycz, M.J., Lein, E.S., Guillozet-Bongaarts, A.L., Shen, E.H., Ng, L., Miller, J.A., van de Lagemaat, L.N., Smith, K.A., Ebbert, A., Riley, Z.L., Abajian, C., Beckmann, C.F., Bernard, A., Bertagnoli, D., Boe, A.F., Cartagena, P.M., Chakravarty, M.M., Chapin, M., Chong, J., Dalley, R.A., Daly, B.D., Dang, C., Datta, S., Dee, N., Dolbeare, T.A., Faber, V., Feng, D., Fowler, D.R., Goldy, J., Gregor, B.W., Haradon, Z., Haynor, D.R., Hohmann, J.G., Horvath, S., Howard, R.E., Jeromin, A., Jochim, J.M., Kinnunen, M., Lau, C., Lazarz, E.T., Lee, C., Lemon, T.A., Li, L., Li, Y., Morris, J.A., Overly, C.C., Parker, P.D., Parry, S.E., Reding, M., Royall, J.J., Schulkun, J., Sequeira, P.A., Slaughterbeck, C.R., Smith, S.C., Sodt, A.J., Sunkin, S.M., Swanson, B.E., Vawter, M.P., Williams, D., Wahnoutka, P., Zielke, H.R., Geschwind, D.H., Hof, P.R., Smith, S.M., Koch, C., Grant, S.G., Jones, A.R., 2012. An anatomically comprehensive atlas of the adult human brain transcriptome. *Nature* 489, 391–399.
- Horvath, S., Zhang, B., Carlson, M., Lu, K.V., Zhu, S., Felciano, R.M., Laurance, M.F., Zhao, W., Qi, S., Chen, Z., Lee, Y., Scheek, A.C., Liao, L.M., Wu, H., Geschwind, D.H., Febbo, P.G., Kornblum, H.I., Cloughesy, T.F., Nelson, S.F., Mischel, P.S., 2006. Analysis of oncogenic signaling networks in glioblastoma identifies ASPM as a molecular target. *Proc. Natl. Acad. Sci. U. S. A.* 103, 17402–17407.
- Jensen, C.J., Massie, A., De Keyser, J., 2013. Immune players in the CNS: the astrocyte. *J. Neuroimmunol. Pharmacol.* 8, 824–839.
- Lambert, J.C., Heath, S., Even, G., Campion, D., Sleegers, K., Hiltunen, M., Combarros, O., Zelenika, D., Bullido, M.J., Tavernier, B., Letenneur, L., Bettens, K., Berr, C., Pasquier, F., Fiévet, N., Barberger-Gateau, P., Engelborghs, S., De Deyn, P., Mateo, I., Franck, A., Helisalmi, S., Porcellini, E., Hanon, O., European Alzheimer's Disease Initiative Investigators, de Pancorbo, M.M., Lendon, C., Dufouil, C., Jaillard, C., Leveillard, T., Alvarez, V., Bosco, P., Mancuso, M., Panza, F., Nacmias, B., Bossù, P., Piccardi, P., Annini, G., Seripa, D., Galimberti, D., Hannequin, D., Licastro, F., Soininen, H., Ritchie, K., Blanché, H., Dartigues, J.F., Tzourio, C., Gut, I., Van Broeckhoven, C., Alperovitch, A., Lathrop, M., Amouyel, P., 2009. Genome-wide association study identifies variants at CLU and CR1 associated with Alzheimer's disease. *Nat. Genet.* 41, 1094–1099.
- Landfield, P.W., Rose, G., Sandles, L., Wohlstaetter, T.C., Lynch, G., 1977. Patterns of astroglial hypertrophy and neuronal degeneration in the hippocampus of ages, memory-deficient rats. *J. Gerontol.* 32, 3–12.
- Liang, W.S., Dunkley, T., Beach, T.G., Grover, A., Mastroeni, D., Ramsey, K., Caselli, R.J., Kukull, W.A., McKeel, D., Morris, J.C., Hulette, C.M., Schmechel, D., Reiman, E.M., Rogers, J., Stephan, D.A., 2008a. Altered neuronal gene expression in brain regions differentially affected by Alzheimer's disease: a reference data set. *Physiol. Genomics* 33, 240–256.
- Liang, W.S., Dunkley, T., Beach, T.G., Grover, A., Mastroeni, D., Ramsey, K., Caselli, R.J., Kukull, W.A., McKeel, D., Morris, J.C., Hulette, C.M., Schmechel, D., Reiman, E.M., Rogers, J., Stephan, D.A., 2010. Neuronal gene expression in non-demented individuals with intermediate Alzheimer's disease neuropathology. *Neurobiol. Aging* 31, 549–566.
- Liang, W.S., Reiman, E.M., Valla, J., Dunkley, T., Beach, T.G., Grover, A., Niedzielko, T.L., Schneider, L.E., Mastroeni, D., Caselli, R., Kukull, W., Morris, J.C., Hulette, C.M., Schmechel, D., Rogers, J., Stephan, D.A., 2008b. Alzheimer's disease is associated with reduced expression of energy metabolism genes in posterior cingulate neurons. *Proc. Natl. Acad. Sci. U. S. A.* 105, 4441–4446.

- Loring, J.F., Wen, X., Lee, J.M., Seilhamer, J., Somogyi, R., 2001. A gene expression profile of Alzheimer's disease. *DNA Cell Biol.* 20, 683–695.
- Magistretti, P.J., Pellerin, L., 1996. Cellular bases of brain energy metabolism and their relevance to functional brain imaging: evidence for a prominent role of astrocytes. *Cereb. Cortex* 6, 50–61.
- Mark, R.J., Pang, Z., Geddes, J.W., Uchida, K., Mattson, M.P., 1997. Amyloid beta-peptide impairs glucose transport in hippocampal and cortical neurons: involvement of membrane lipid peroxidation. *J. Neurosci.* 17, 1046–1054.
- Matsuda, S., Matsuda, Y., D'Adamo, L., 2009. CD74 interacts with APP and suppresses the production of A β . *Mol. Neurodegener.* 4, 41.
- McKhann, G., Drachman, D., Folstein, M., Katzman, R., Price, D., Stadlan, E.M., 1984. Clinical diagnosis of Alzheimer's disease: report of the NINCDS-ADRDA Work Group under the auspices of Department of Health and Human Services Task Force on Alzheimer's Disease. *Neurology* 34, 939–944.
- Minoshima, S., Giordani, B., Berent, S., Frey, K.A., Foster, N.L., Kuhl, D.E., 1997. Metabolic reduction in the posterior cingulate cortex in very early Alzheimer's disease. *Ann. Neurol.* 42, 85–94.
- Mulder, S.D., Nielsen, H.M., Blankenstein, M.A., Eikelenboom, P., Veerhuis, R., 2014. Apolipoproteins E and J interfere with amyloid-beta uptake by primary human astrocytes and microglia in vitro. *Glia* 62, 493–503.
- Nedergaard, M., Ransom, B., Goldman, S.A., 2003. New roles for astrocytes: redefining the functional architecture of the brain. *Trends Neurosci.* 26, 523–530.
- Orre, M., Kamphuis, W., Osborn, L.M., Melief, J., Kooijman, L., Huitinga, I., Klooster, J., Bossers, K., Hol, E.M., 2014. Acute isolation and transcriptome characterization of cortical astrocytes and microglia from young and aged mice. *Neurobiol. Aging* 35, 1–14.
- Pagliarini, D.J., Calvo, S.E., Chang, B., Sheth, S.A., Vafai, S.B., Ong, S.E., Walford, G.A., Sugiana, C., Boneh, A., Chen, W.K., Hill, D.E., Vidal, M., Evans, J.G., Thorburn, D.R., Carr, S.A., Mootha, V.K., 2008. A mitochondrial protein compendium elucidates complex I disease biology. *Cell* 134, 112–123.
- Panther, S.S., McSwigan, J.D., Sheppard, J.R., Emory, C.R., Frey 2nd, W.H., 1985. Glial fibrillary acidic protein and Alzheimer's disease. *Neurochem. Res.* 10, 1567–1576.
- Pasternack, J.M., Abraham, C.R., Van Dyke, B.J., Potter, H., Younkin, S.G., 1989. Astrocytes in Alzheimer's disease gray matter express alpha 1-antichymotrypsin mRNA. *Am. J. Pathol.* 135, 827–834.
- Pekny, M., Leveen, P., Pekna, M., Eliasson, C., Berthold, C.H., Westermarck, B., Betsholtz, C., 1995. Mice lacking glial fibrillary acidic protein display astrocytes devoid of intermediate filaments but develop and reproduce normally. *Embo J* 14, 1590–1598.
- Pekny, M., Pekna, M., 2004. Astrocyte intermediate filaments in CNS pathologies and regeneration. *J. Pathol.* 204, 428–437.
- Pellerin, L., Magistretti, P.J., 1994. Glutamate uptake into astrocytes stimulates aerobic glycolysis: a mechanism coupling neuronal activity to glucose utilization. *Proc. Natl. Acad. Sci. U. S. A.* 91, 10625–10629.
- Perez-Nievas, B.G., Stein, T.D., Tai, H.C., Dols-Icardo, O., Scotton, T.C., Barroeta-Espar, I., Fernandez-Carballo, L., de Munain, E.L., Perez, J., Marquie, M., Serrano-Pozo, A., Frosch, M.P., Lowe, V., Parisi, J.E., Petersen, R.C., Ikonomic, M.D., López, O.L., Klunk, W., Hyman, B.T., Gómez-Isla, T., 2013. Dissecting phenotypic traits linked to human resilience to Alzheimer's pathology. *Brain* 136 (Pt 8), 2510–2526.
- Piert, M., Koeppe, R.A., Giordani, B., Berent, S., Kuhl, D.E., 1996. Diminished glucose transport and phosphorylation in Alzheimer's disease determined by dynamic FDG-PET. *J. Nucl. Med.* 37, 201–208.
- Poliseno, L., 2012. Pseudogenes: newly discovered players in human cancer. *Sci. Signal* 5, re5.
- Reichwald, J., Danner, S., Wiederhold, K.H., Staufenbiel, M., 2009. Expression of complement system components during aging and amyloid deposition in APP transgenic mice. *J. Neuroinflammation* 6, 35.
- Reiman, E.M., Caselli, R.J., Chen, K., Alexander, G.E., Bandy, D., Frost, J., 2001. Declining brain activity in cognitively normal apolipoprotein E epsilon 4 heterozygotes: a foundation for using positron emission tomography to efficiently test treatments to prevent Alzheimer's disease. *Proc. Natl. Acad. Sci. U. S. A.* 98, 3334–3339.
- Reiman, E.M., Caselli, R.J., Yun, L.S., Chen, K., Bandy, D., Minoshima, S., Thibodeau, S.N., Osborne, D., 1996. Preclinical evidence of Alzheimer's disease in persons homozygous for the epsilon 4 allele for apolipoprotein E. *N. Engl. J. Med.* 334, 752–758.
- Reiman, E.M., Chen, K., Alexander, G.E., Caselli, R.J., Bandy, D., Osborne, D., Saunders, A.M., Hardy, J., 2004. Functional brain abnormalities in young adults at genetic risk for late-onset Alzheimer's dementia. *Proc. Natl. Acad. Sci. U. S. A.* 101, 284–289.
- Roelofs, R.F., Fischer, D.F., Houtman, S.H., Sluijs, J.A., Van Haren, W., Van Leeuwen, F.W., Hol, E.M., 2005. Adult human subventricular, subgranular, and subpial zones contain astrocytes with a specialized intermediate filament cytoskeleton. *Glia* 52, 289–300.
- Schwartz, W.J., Smith, C.B., Davidsen, L., Savaki, H., Sokoloff, L., Mata, M., Fink, D.J., Gainer, H., 1979. Metabolic mapping of functional activity in the hypothalamo-neurohypophyseal system of the rat. *Science* 205, 723–725.
- Sherwood, C.C., Stimpson, C.D., Raghanti, M.A., Wildman, D.E., Uddin, M., Grossman, L.L., Goodman, M., Redmond, J.C., Bonar, C.J., Erwin, J.M., Hof, P.R., 2006. Evolution of increased glia-neuron ratios in the human frontal cortex. *Proc. Natl. Acad. Sci. U. S. A.* 103, 13606–13611.
- Simpson, J.E., Ince, P.G., Shaw, P.J., Heath, P.R., Raman, R., Garwood, C.J., Gelsthorpe, C., Baxter, L., Forster, G., Matthews, F.E., Brayne, C., Wharton, S.B., MRC Cognitive Function and Ageing Neuropathology Study Group, 2011. Microarray analysis of the astrocyte transcriptome in the aging brain: relationship to Alzheimer's pathology and APOE genotype. *Neurobiol. Aging* 32, 1795–1807.
- Sofroniew, M.V., 2009. Molecular dissection of reactive astrogliosis and glial scar formation. *Trends Neurosci.* 32, 638–647.
- Sofroniew, M.V., Vinters, H.V., 2010. Astrocytes: biology and pathology. *Acta Neuropathol.* 119, 7–35.
- Tello, D., Balsa, E., Acosta-Iborra, B., Fuertes-Yebra, E., Elorza, A., Ordóñez, A., Corral-Escariz, M., Soro, I., López-Bernardo, E., Perales-Clemente, E., Martínez-Ruiz, A., Enríquez, J.A., Aragón, J., Cadenas, S., Landázuri, M.O., 2011. Induction of the mitochondrial NDUFA4L2 protein by HIF-1 α decreases oxygen consumption by inhibiting complex I activity. *Cell Metab* 14, 768–779.
- Thal, L.J., Kantarci, K., Reiman, E.M., Klunk, W.E., Weiner, M.W., Zetterberg, H., Galasko, D., Praticò, D., Griffin, S., Schenk, D., Siemers, E., 2006. The role of biomarkers in clinical trials for Alzheimer disease. *Alzheimer Dis. Assoc. Disord* 20, 6–15.
- Trapnell, C., Pachter, L., Salzberg, S.L., 2009. TopHat: discovering splice junctions with RNA-Seq. *Bioinformatics* 25, 1105–1111.
- Trapnell, C., Roberts, A., Goff, L., Pertea, G., Kim, D., Kelley, D.R., Pimentel, H., Salzberg, S.L., Rinn, J.L., Pachter, L., 2012. Differential gene and transcript expression analysis of RNA-seq experiments with TopHat and cufflinks. *Nat. Protoc.* 7, 562–578.
- Tsacopoulos, M., Magistretti, P.J., 1996. Metabolic coupling between glia and neurons. *J. Neurosci.* 16, 877–885.
- Valla, J., Berndt, J.D., Gonzalez-Lima, F., 2001. Energy hypometabolism in posterior cingulate cortex of Alzheimer's patients: superficial laminar cytochrome oxidase associated with disease duration. *J. Neurosci.* 21, 4923–4930.
- Woischnik, M., Moraes, C.T., 2002. Pattern of organization of human mitochondrial pseudogenes in the nuclear genome. *Genome Res.* 12, 885–893.
- Yasui, D.H., Xu, H., Dunaway, K.W., Lasalle, J.M., Jin, L.W., Maezawa, I., 2013. MeCP2 modulates gene expression pathways in astrocytes. *Mol. Autism* 4, 3.
- Yeung, K.T., Das, S., Zhang, J., Lomniczi, A., Ojeda, S.R., Xu, C.F., Neubert, T.A., Samuels, H.H., 2011. A novel transcription complex that selectively modulates apoptosis of breast cancer cells through regulation of FASTKD2. *Mol. Cell Biol* 31, 2287–2298.
- Zhang, B., Horvath, S., 2005. A general framework for weighted gene co-expression network analysis. *Stat. Appl. Genet. Mol. Biol.* 4, 4.
- Zhao, J., O'Connor, T., Vassar, R., 2011. The contribution of activated astrocytes to A β production: implications for Alzheimer's disease pathogenesis. *J. Neuroinflammation* 8, 150.